Oncology Advances **2026** vol. 4(2) | e00003
DOI: 10.14218/OnA.2026.00003

Original Article

Multi-omics Analysis of *TMED3* as a Potential Prognostic Biomarker Across Six Cancer Types

Zhui Ke[1], Peng Ji[1], Jingyi Lu[2], Yongqing Yang[3], Xianling Guo[2], Yue Li[2] and Lan Chen[4*]

[1]*Department of Critical Care Medicine, Xiangshui County People's Hospital, Yancheng, Jiangsu, China;* [2]*Department of Oncology, Shanghai Tenth People's Hospital Affiliated to Tongji University, Shanghai, China;* [3]*Department of Orthopedics, Jinjiang Municipal Hospital (Fujian Hospital of Shanghai Sixth People's Hospital), Jinjiang, Fujian, China;* [4]*School of Clinical Medicine, Anhui University of Science and Technology, Huainan, Anhui, China*

Received: February 07, 2026 | **Revised:** April 10, 2026 | **Accepted:** June 15, 2026 | **Published online:** June 28, 2026

Abstract

Background and objectives: The clinical and genetic characteristics of TMED3, a p24-family protein, across different cancer types remain incompletely understood. This study aimed to evaluate its expression patterns, prognostic relevance, epigenetic regulation, immune associations, genetic alterations, functional networks, and chemical-gene interactions across six cancer types.

Methods: Public, de-identified data from UALCAN, GENT2, the Human Protein Atlas (HPA), Kaplan-Meier Plotter, MEXPRESS, cBioPortal, TIMER2.0, the Comparative Toxicogenomics Database (CTD), STRING, and DAVID were analyzed. The clinical and genetic characteristics of *TMED3* in bladder cancer (BLCA), head and neck squamous cell carcinoma (HNSC), kidney renal clear cell carcinoma (KIRC), kidney renal papillary cell carcinoma (KIRP), liver hepatocellular carcinoma (LIHC), and lung adenocarcinoma (LUAD) were analyzed. Database-reported nominal *P*-values were used because unified multiple-testing correction was not feasible.

Results: In UALCAN analysis, *TMED3* mRNA was upregulated in BLCA, KIRP, LIHC, KIRC, and LUAD and downregulated in HNSC. HPA data showed higher TMED3 protein expression in BLCA, HNSC, and LUAD. Kaplan-Meier Plotter analysis showed that higher *TMED3* expression was associated with shorter overall survival in HNSC, KIRC, KIRP, LIHC, and LUAD, but not in BLCA, and was not significantly associated with recurrence-free survival in any of the six cancers. MEXPRESS analysis suggested an inverse association between promoter methylation and *TMED3* expression. TIMER analysis showed negative correlations between *TMED3* expression and $CD8^+$ T-cell infiltration in BLCA, HNSC, and LUAD, but a positive correlation in LIHC. cBioPortal showed low *TMED3* alteration frequencies across the six cancers, and STRING and DAVID analyses linked *TMED3*-associated genes mainly to endoplasmic reticulum-Golgi trafficking and vesicle-mediated transport pathways. CTD analysis identified azacitidine, doxorubicin, and MK-2206 as chemicals associated with altered *TMED3* expression.

Conclusions: *TMED3* is a cancer-type-specific prognostic candidate associated with shorter overall survival in five of the six analyzed cancers. Its transcript-protein discordance, methylation pattern, and immune correlations define testable biological hypotheses, but independent experimental and clinical validation is required before clinical application.

Introduction

Cancer remains a major global health challenge,[1] and the identification of robust molecular biomarkers is essential for improving risk stratification, prognostic assessment, and individualized treatment. Although many molecular markers have been proposed, their applicability across tumor types is often limited by tumor heterogeneity, database-specific effects, and insufficient biological validation. Therefore, integrative analyses that combine transcriptomic, protein-level, epigenetic, genomic, immune, and pharmacological information may help prioritize candidate biomarkers for subsequent experimental and clinical validation.

The transmembrane emp24 domain-containing protein (TMED)/p24 family participates in vesicular transport between the Golgi ap-

Keywords: *TMED3*; Cross-cancer analysis; Multi-omics; Prognostic biomarker; Promoter methylation; Copy number variation; $CD8^+$ T-cell infiltration; Chemical-gene interaction network.

***Correspondence to:** Lan Chen, School of Clinical Medicine, Anhui University of Science and Technology, Huainan, Anhui 232001, China. ORCID: https://orcid.org/0009-0005-1793-6387. Tel: +86-15872747680, E-mail: cl17355482561@163.com

How to cite this article: Ke Z, Ji P, Lu J, Yang Y, Guo X, Li Y, *et al*. Multi-omics Analysis of *TMED3* as a Potential Prognostic Biomarker Across Six Cancer Types. *Oncol Adv* 2026;4(2):e00003. doi: 10.14218/OnA.2026.00003.

paratus and the endoplasmic reticulum (ER) and contributes to secretory pathway homeostasis.[2,3] TMED3, a member of the p24 protein family, has been implicated in unconventional protein secretion and cancer-related signaling. Previous studies have suggested that TMED3 may function either as an oncogenic factor or as a tumor suppressor depending on tumor context.[4–6] More recent mechanistic studies further indicate that TMED3 can promote malignant phenotypes in ovarian cancer, prostate cancer, and glioma through pathways involving SMAD2, FOXO1a/FOXO3a phosphorylation, and ZBTB7A signaling.[7–9] These findings provide a biological rationale for evaluating whether *TMED3* has broader prognostic relevance across cancer types.

Therefore, the aim of the present study was to evaluate the expression pattern, prognostic significance, promoter methylation, genetic alterations, copy number variations (CNVs), protein–protein interactions (PPI), $CD8^+$ T-cell infiltration, and Comparative Toxicogenomics Database (CTD)-derived chemical-gene interactions of *TMED3* across six cancer types, including bladder cancer (BLCA), head and neck squamous cell carcinoma (HNSC), kidney renal clear cell carcinoma (KIRC), kidney renal papillary cell carcinoma (KIRP), liver hepatocellular carcinoma (LIHC), and lung adenocarcinoma (LUAD). Because this was an exploratory computational study, all associations were interpreted as candidates requiring independent validation.

Materials and methods

All databases were accessed between January 1, 2022 and June 1, 2026.

UALCAN database analysis

The UALCAN database (http://ualcan.path.uab.edu) was used to compare *TMED3* transcript expression levels across multiple human cancers and their corresponding normal tissues to evaluate differential expression.[10,11]

Kaplan-Meier Plotter database analysis

In this study, the Kaplan-Meier Plotter database (http://kmplot.com/analysis) was employed to evaluate the association between TMED3 expression levels and overall survival (OS) as well as recurrence-free survival (RFS) in patients with six selected cancer types.[12]

The optimal cutoff value was determined using the "auto select best cutoff" function to maximize survival differences between groups, and hazard ratios (HRs), 95% confidence intervals (CIs), and log-rank P-values were recorded.

GENT2 database analysis

The GENT2 database (http://gent2.appex.kr/) integrates public gene expression datasets to systematically compare gene expression profiles between normal and tumor tissues.[13]

Human Protein Atlas (HPA) database analysis

HPA (https://www.proteinatlas.org/) is a public database integrating antibody-based immunohistochemistry, transcriptomic, and proteomic data to reveal protein expression patterns in normal and cancer tissues.[14,15] The HPA database was used to evaluate TMED3 protein expression levels in normal tissues and different cancers. Based on immunohistochemistry staining intensity and the proportion of positive cells, TMED3 protein expression was semi-quantitatively classified into four levels: not detected, low, medium, and high.

MEXPRESS database analysis

The MEXPRESS database (https://www.mexpress.be) was used to evaluate the correlation between *TMED3* transcript expression and promoter methylation levels in 450 BLCA, 612 HNSC, 980 KIRC, 380 KIRP, 468 LIHC, and 861 LUAD tumor samples.[16]

cBioPortal database analysis

CNVs and other genetic alterations of *TMED3* across the selected cancer subtypes were analyzed using the cBioPortal for Cancer Genomics database.[17,18] Alteration types, including missense mutations, amplification, and deep deletion, were summarized descriptively.

PPI network construction and pathway analysis

TMED3-interacting proteins were screened using STRING (Homo sapiens, confidence ≥ 0.400), with the PPI network visualized via Cytoscape (https://string-db.org/).[19,20] GO and KEGG enrichment analyses were performed using DAVID (Homo sapiens, adjusted $P < 0.05$) (https://davidbioinformatics.nih.gov/).[21]

Analysis of TMED3 expression and $CD8^+$ T-cell immune infiltration levels

Immune cell infiltration levels were analyzed using the TIMER2.0 database (http://timer.cistrome.org/). The abundance of immune cells was estimated using the CIBERSORT-ABS algorithm, and Spearman correlation analysis was performed to evaluate the relationship between TMED3 expression and $CD8^+$ T-cell infiltration levels across multiple cancer types.[22]

Chemical-gene interaction network analysis

The CTD (http://ctdbase.org/) links toxicological information on chemicals, genes, phenotypes, diseases, and exposures.[23] A *TMED3*-related chemical-gene interaction network was constructed using CTD and Cytoscape software. Because CTD-derived chemical-gene relationships are based on curated associations from existing studies, the analysis was considered exploratory and was not interpreted as direct evidence of drug efficacy in *TMED3*-high tumors.

Statistical methods

Differential expression analysis was performed using the UALCAN (TPM values) and GENT2 (normalized expression profiles) databases. Student's t-test was used to compare *TMED3* expression levels between tumor and normal tissues when provided by the source database. Correlation analysis was conducted using MEXPRESS to evaluate the association between *TMED3* mRNA expression and promoter methylation and using TIMER to assess the association between *TMED3* expression and $CD8^+$ T-cell infiltration. Survival analysis was performed using the Kaplan-Meier Plotter database to assess OS and RFS, with intergroup comparisons conducted using the log-rank test. Genetic alteration analysis was performed using cBioPortal to describe the frequency and type of *TMED3* mutations and CNVs. Functional enrichment analysis was conducted using DAVID. The analyses relied on database-reported nominal *P*-values. Raw result matrices required to calculate adjusted q-values across all tested comparisons were not consistently available from the public database outputs; therefore, adjusted q-values were not calculated or reported. Accordingly, $P < 0.05$ was treated as a nominal significance threshold, and findings involving multiple comparisons should be interpreted as exploratory rather than confirmatory.

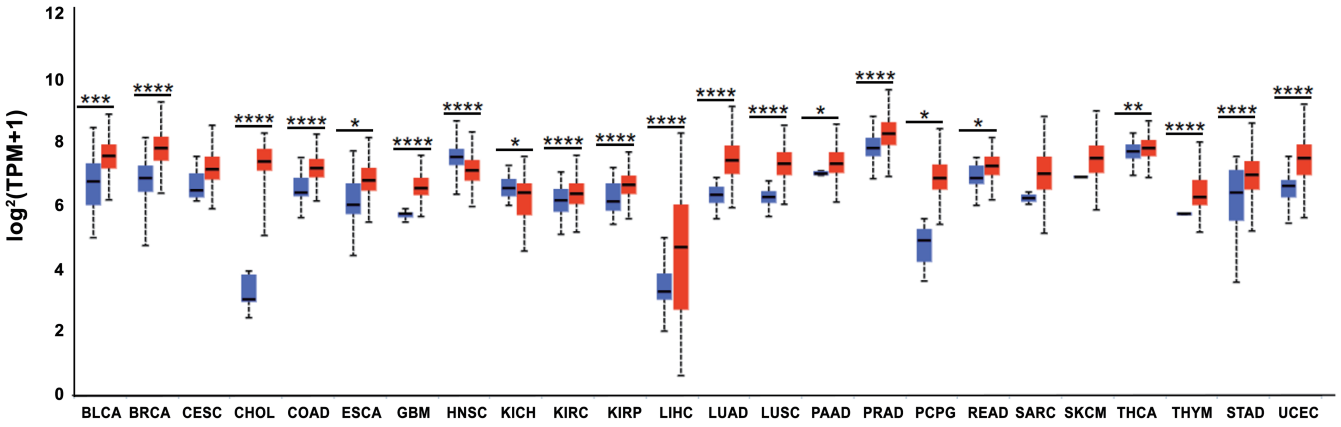

Fig. 1. *TMED3* transcript expression in tumor and corresponding normal tissues in UALCAN/TCGA. Red boxes represent tumor samples, and blue boxes represent normal samples. Cancer abbreviations follow TCGA nomenclature. The central line indicates the median, boxes indicate the interquartile range, and whiskers/outliers show the distribution provided by UALCAN. *$P < 0.05$, **$P < 0.01$, ***$P < 0.001$, and ****$P < 0.0001$ for tumor-versus-normal comparisons. BLCA, bladder cancer; BRCA, breast cancer; CESC, cervical squamous cell carcinoma and endocervical adenocarcinoma; CHOL, cholangiocarcinoma; COAD, colon adenocarcinoma; ESCA, esophageal carcinoma; GBM, glioblastoma multiforme; HNSC, head and neck squamous cell carcinoma; KICH, kidney chromophobe; KIRC, kidney renal clear cell carcinoma; KIRP, kidney renal papillary cell carcinoma; LIHC, liver hepatocellular carcinoma; LUAD, lung adenocarcinoma; LUSC, lung squamous cell carcinoma; PAAD, pancreatic adenocarcinoma; PCPG, pheochromocytoma and paraganglioma; PRAD, prostate adenocarcinoma; READ, rectum adenocarcinoma; SARC, sarcoma; SKCM, skin cutaneous melanoma; STAD, stomach adenocarcinoma; TCGA, The Cancer Genome Atlas; THCA, thyroid carcinoma; THYM, thymoma; TPM, transcripts per million; UCEC, uterine corpus endometrial carcinoma.

Results

TMED3 transcriptional expression in human cancers and normal tissues

In this study, transcriptional expression levels of *TMED3* across 24 major human cancer subtypes were analyzed using the UALCAN database based on The Cancer Genome Atlas dataset. The results revealed that *TMED3* mRNA expression levels were significantly higher in BLCA, KIRP, LIHC, LUAD, and KIRC compared with their corresponding adjacent normal tissues. Conversely, *TMED3* expression was significantly downregulated in HNSC relative to normal tissues ($P < 0.05$) (Fig. 1).

Prognostic potential of TMED3 in multiple cancers

To further evaluate the prognostic value of *TMED3* expression, associations between *TMED3* expression levels and OS as well as RFS were analyzed in six cancer types (Fig. 2). In BLCA, neither OS (HR = 1.22, 95% CI: 0.88–1.68, $P > 0.05$) nor RFS (HR = 1.67, 95% CI: 0.78–3.55, $P > 0.05$) showed a statistically significant association. In HNSC, OS was significantly associated with *TMED3* expression (HR = 1.52, 95% CI: 1.16–1.99, $P < 0.05$), whereas RFS was not (HR = 1.99, 95% CI: 0.76–5.24, $P > 0.05$). In KIRC, OS showed a significant association (HR = 1.77, 95% CI: 1.32–2.39, $P < 0.05$), while RFS did not (HR = 5.22, 95% CI: 0.69–39.75, $P > 0.05$). In KIRP, OS was significantly correlated with *TMED3* expression (HR = 2.46, 95% CI: 1.26–4.79, $P < 0.05$), but RFS was not (HR = 1.95, 95% CI: 0.91–4.17, $P > 0.05$). In LIHC, OS showed a significant association (HR = 1.49, 95% CI: 1.05–2.11, $P < 0.05$), whereas RFS did not (HR = 0.89, 95% CI: 0.62–1.30, $P > 0.05$). In LUAD, OS was significantly associated with *TMED3* expression (HR = 1.56, 95% CI: 1.09–2.21, $P < 0.05$), while RFS did not reach statistical significance (HR = 1.50, 95% CI: 0.98–2.31, $P > 0.05$).

Overall, elevated *TMED3* expression was associated with a trend toward shorter OS across the six cancer types analyzed. This association reached nominal statistical significance in HNSC, KIRC, KIRP, LIHC, and LUAD ($P < 0.05$), but not in BLCA. In contrast, RFS did not reach nominal statistical significance in any of the six cancer types; therefore, RFS-related findings were interpreted cautiously and were not described as statistically significant.

Correlation of TMED3 expression with clinicopathological features in six cancer types

This study analyzed *TMED3* transcriptional expression in BLCA, HNSC, KIRC, KIRP, LIHC, and LUAD and examined associations with clinicopathological features, including tumor stage, race, sex, and age subgroup. In BLCA, *TMED3* was significantly upregulated in stages II–IV, in Caucasian and Asian patients, in males and females, and in the 41–60 and 61–80 year age groups compared with normal controls ($P < 0.01$), whereas stage I, African American, and 21–40 year subgroups did not reach statistical significance, likely in part due to small sample sizes. In HNSC, *TMED3* was significantly downregulated across most clinicopathological subgroups ($P < 0.05$). In KIRC, subgroup-level results differed from the overall UALCAN tumor–normal comparison, suggesting that KIRC findings should be interpreted cautiously and verified in independent cohorts. In KIRP, LIHC, and LUAD, *TMED3* was generally upregulated in most evaluated subgroups ($P < 0.05$), although several subgroups with limited sample sizes did not reach statistical significance.

In summary, *TMED3* dysregulation was observed across multiple clinicopathological subgroups; however, the direction and robustness of this dysregulation varied by cancer type and subgroup. These findings support further investigation of *TMED3* while emphasizing the need for independent validation.

Validation of TMED3 transcriptional levels using independent cohorts

TMED3 transcriptional expression in BLCA, HNSC, KIRC, KIRP, LIHC, and LUAD was further evaluated using the GENT2 database. Compared with normal tissues, *TMED3* was significantly upregulated in BLCA, KIRC, KIRP, LIHC, and LUAD ($P < 0.05$), whereas it was downregulated in HNSC ($P < 0.05$) (Fig. 3). Al-

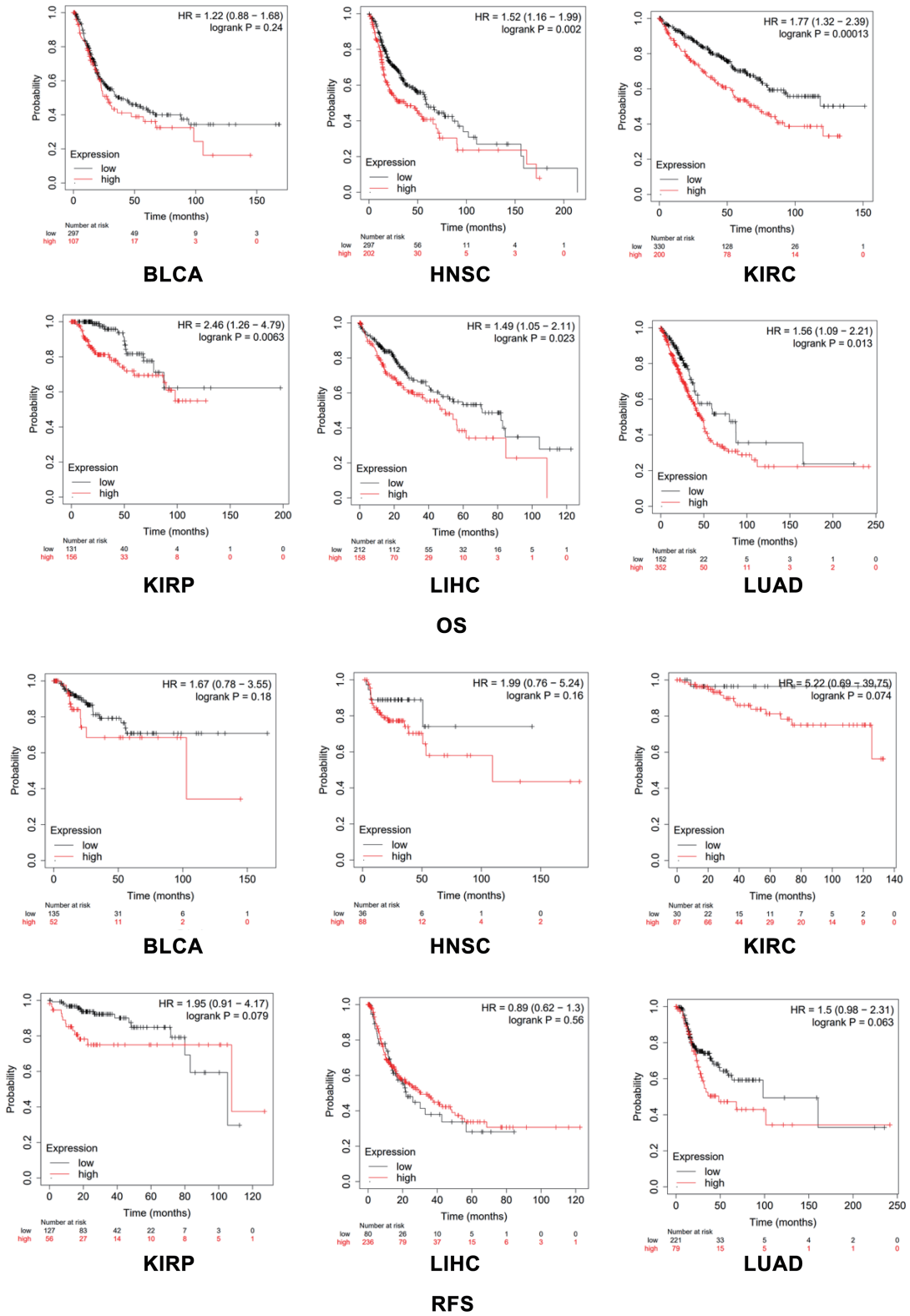

Fig. 2. Association between *TMED3* expression and overall survival (OS) or recurrence-free survival (RFS) in different tumor subtypes. $P < 0.05$ was considered nominally significant based on database-reported values; adjusted q-values were not available, and survival associations should therefore be interpreted as exploratory. BLCA, bladder cancer; CI, confidence interval; HNSC, head and neck squamous cell carcinoma; HR, hazard ratio; KIRC, kidney renal clear cell carcinoma; KIRP, kidney renal papillary cell carcinoma; LIHC, liver hepatocellular carcinoma; LUAD, lung adenocarcinoma; OS, overall survival; RFS, recurrence-free survival.

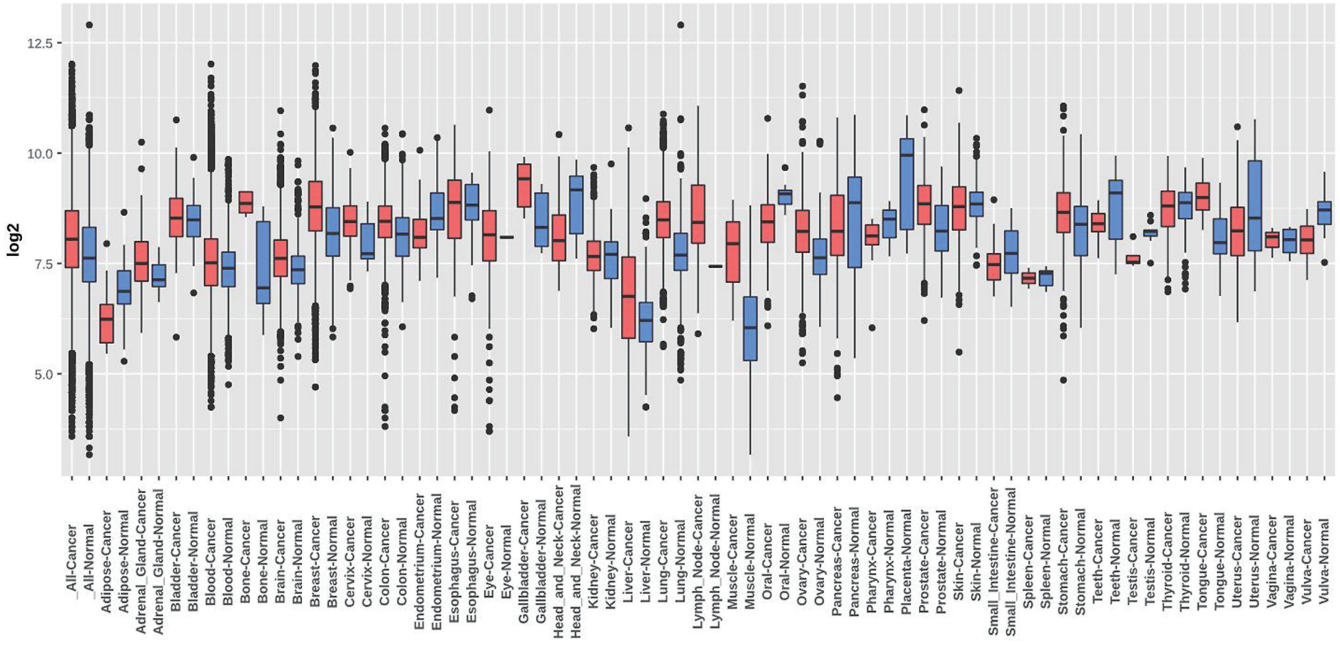

Fig. 3. Validation of *TMED3* transcriptional expression in BLCA, HNSC, KIRC, KIRP, LIHC, and LUAD using the GENT2 database. Blue indicates normal samples, and red indicates tumor samples. $P < 0.05$ was considered nominally significant based on database-reported values. BLCA, bladder cancer; HNSC, head and neck squamous cell carcinoma; KIRC, kidney renal clear cell carcinoma; KIRP, kidney renal papillary cell carcinoma; LIHC, liver hepatocellular carcinoma; LUAD, lung adenocarcinoma.

though KIRC showed increased *TMED3* expression in both the UALCAN and GENT2 analyses, subgroup-level results were not fully consistent; therefore, these findings should be interpreted cautiously and validated in independent cohorts.

Analysis of TMED3 protein expression levels

TMED3 protein expression in cancer and normal tissues of BLCA, HNSC, KIRC, KIRP, LIHC, and LUAD was analyzed using the HPA database. The results showed that, compared with corresponding normal tissues, TMED3 protein expression appeared higher in BLCA, HNSC, and LUAD tumor tissues (Fig. 4). In contrast, clear protein-level upregulation of TMED3 was not observed in KIRC, LIHC, or KIRP tumor tissues.

Analysis of TMED3 promoter methylation

Promoter methylation plays a critical role in regulating gene expression and may contribute to cancer-related transcriptional dysregulation. MEXPRESS analysis was used to explore whether *TMED3* expression was associated with promoter methylation levels. The analysis suggested an inverse relationship between *TMED3* promoter methylation and *TMED3* expression in BLCA, HNSC, KIRC, KIRP, LIHC, and LUAD based on database-reported nominal *P*-values. Because methylation–expression analyses involve multiple CpG sites and multiple cancer types, these findings should be regarded as exploratory and should be validated using independent methylation datasets.

Analysis of TMED3 genetic alterations using cBioPortal

Analysis based on the cBioPortal database revealed that, among the six cancer cohorts examined, LUAD exhibited the highest frequency of *TMED3* alterations (1%), characterized primarily by gene amplification and missense mutations (Fig. 5). HNSC followed with an alteration frequency of 0.8%, displaying a heterogeneous pattern comprising missense mutations, amplifications, and deep deletions. In contrast, BLCA and KIRP showed lower alteration frequencies of 0.5% and 0.4%, respectively, while no genetic alterations in *TMED3* were detected in KIRC or LIHC (0%). Collectively, these distribution patterns indicate that the overall frequency of *TMED3* genetic alterations across multiple tumor types is relatively low, suggesting that CNVs are unlikely to be the primary drivers of *TMED3* expression changes in these malignancies.

PPI network construction and pathway enrichment analysis

Enriched genes interacting with *TMED3* were identified using STRING and Cytoscape resources. Functional interaction network analysis revealed that *TMED3* was closely associated with 24 distinct genes (Fig. 6a). Pathways involving *TMED3*-enriched genes were analyzed using the DAVID tool (Fig. 6b).

Functional enrichment analysis of *TMED3*-related genes suggested that TMED3 is connected with proteins involved in ER–Golgi trafficking, p24 family transport functions, cytoskeletal organization, and ARF-family-related vesicle transport. In particular, *TMED2* and *TMED4* were enriched in p24 family protein-related categories, whereas ARF-family members were linked to vesicular transport and Golgi-related regulatory pathways. These results are consistent with the known role of TMED family proteins in secretory pathway regulation and provide a functional context for *TMED3*-associated tumor biology (Fig. 6).

Association between TMED3 expression and $CD8^+$ T-cell infiltration

To investigate whether *TMED3* may be associated with the tumor immune microenvironment, the relationship between *TMED3* expression and $CD8^+$ T-cell infiltration was analyzed in BLCA,

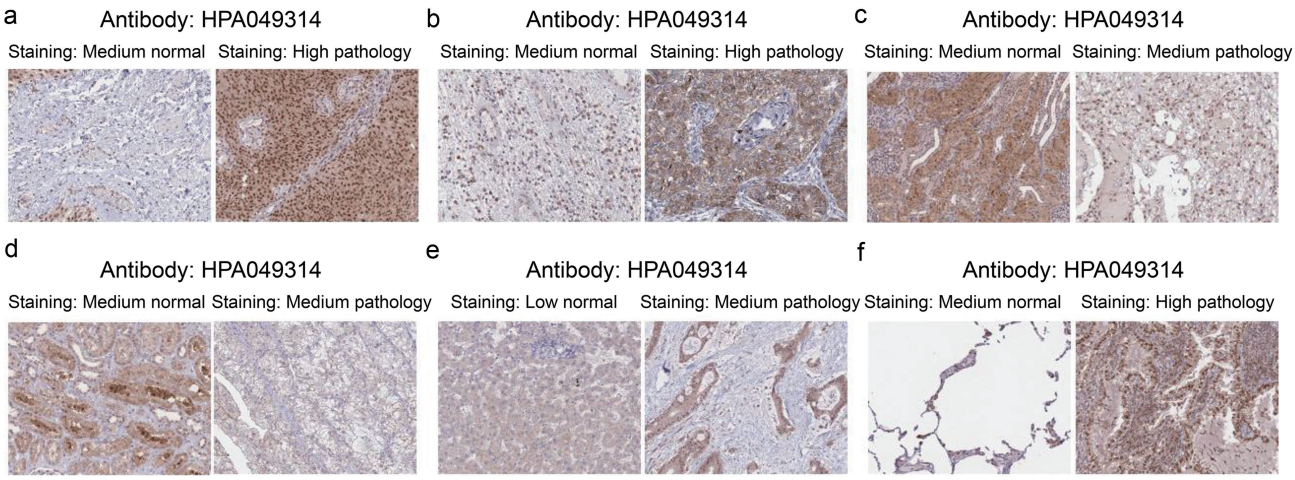

Fig. 4. Representative Human Protein Atlas immunohistochemistry images of TMED3 in normal and tumor tissues. Panels a–f correspond to BLCA, HNSC, KIRC, KIRP, LIHC, and LUAD, respectively; each panel shows normal tissue on the left and corresponding cancer tissue on the right. The staining category reported by HPA is shown beneath each image. Images were obtained from the Human Protein Atlas and are presented for comparative, semi-quantitative assessment. BLCA, bladder cancer; HNSC, head and neck squamous cell carcinoma; HPA, Human Protein Atlas; IHC, immunohistochemistry; KIRC, kidney renal clear cell carcinoma; KIRP, kidney renal papillary cell carcinoma; LIHC, liver hepatocellular carcinoma; LUAD, lung adenocarcinoma.

HNSC, KIRC, KIRP, LIHC, and LUAD using the TIMER database. High *TMED3* expression was significantly negatively correlated with $CD8^+$ T-cell infiltration in BLCA, HNSC, and LUAD. In contrast, correlations in KIRC and KIRP were not statistically significant, whereas LIHC showed a significant positive correlation. These results suggest that the relationship between *TMED3* expression and $CD8^+$ T-cell infiltration is cancer-type specific and cannot be interpreted as uniformly negative across cancers (Fig. 7). Because the analysis is correlational, it cannot establish that TMED3 directly regulates $CD8^+$ T-cell recruitment or function.

Chemical-gene interaction network analysis of TMED3

To explore potential chemical-gene associations involving *TMED3*, a CTD-based chemical-gene interaction network was constructed and visualized using Cytoscape. The results indicated that azacitidine and doxorubicin were associated with increased *TMED3* expression, whereas MK-2206 was associated with decreased *TMED3* expression (Fig. 8). These relationships should be regarded as data-

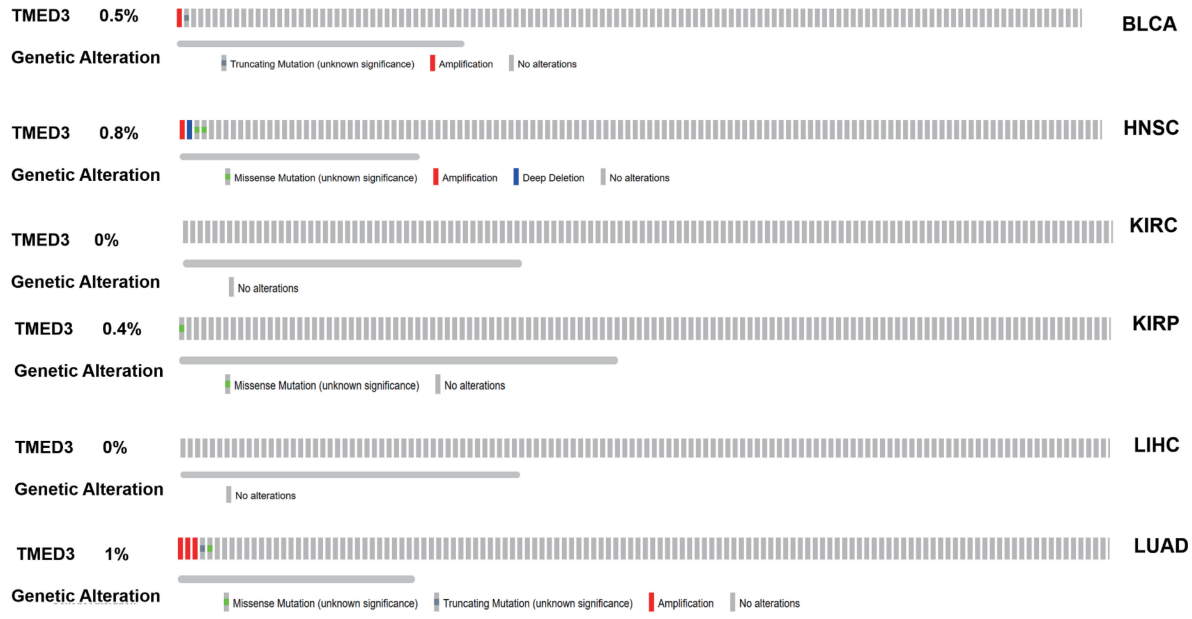

Fig. 5. cBioPortal OncoPrint of *TMED3* genomic alterations in TCGA BLCA, HNSC, KIRC, KIRP, LIHC, and LUAD cohorts. Each column represents one tumor sample, and colored marks indicate the alteration classes shown in the embedded legend, including missense mutation, amplification, and deep deletion; gray indicates no detected alteration. Percentages on the left denote cohort-specific alteration frequencies. The plot shows that *TMED3* alterations are uncommon overall. BLCA, bladder cancer; HNSC, head and neck squamous cell carcinoma; KIRC, kidney renal clear cell carcinoma; KIRP, kidney renal papillary cell carcinoma; LIHC, liver hepatocellular carcinoma; LUAD, lung adenocarcinoma; TCGA, The Cancer Genome Atlas.

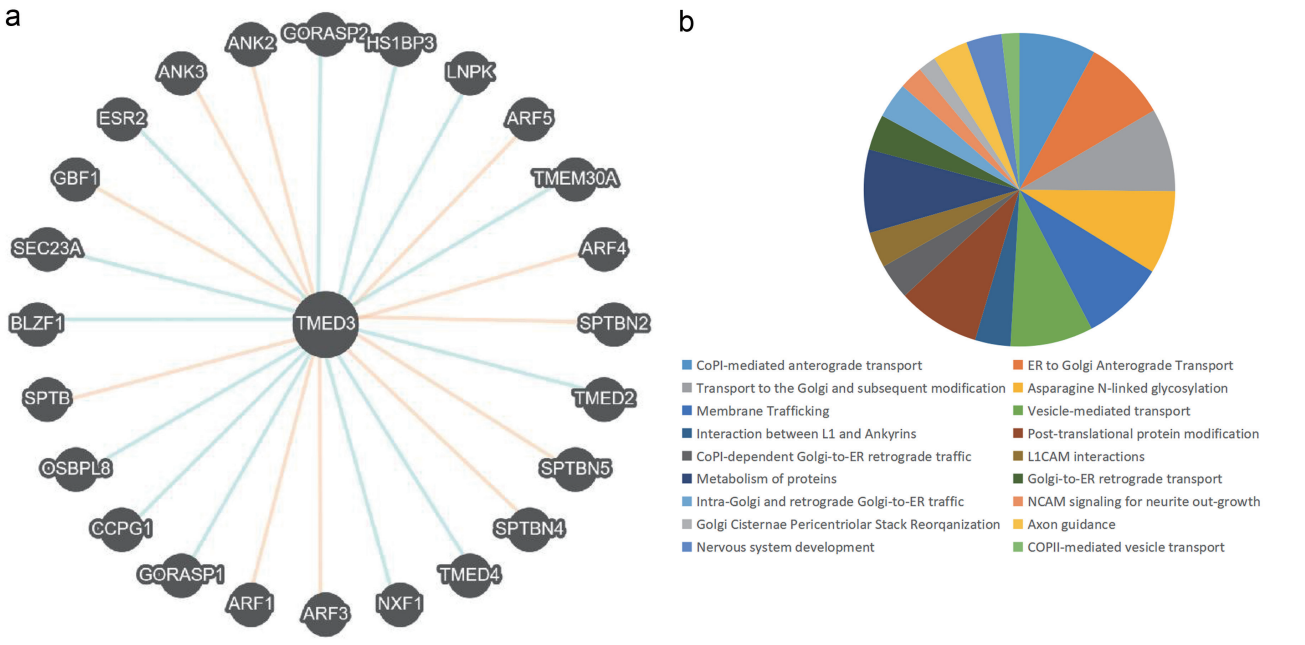

Fig. 6. TMED3 interaction network and functional enrichment. (a) STRING-derived protein–protein interaction network visualized in Cytoscape; nodes represent TMED3 and associated proteins, and edges represent documented or predicted functional interactions. (b) DAVID functional enrichment results for the *TMED3*-associated gene set; colored sectors denote enriched biological processes and pathways, including ER–Golgi trafficking, vesicle-mediated transport, p24 family functions, cytoskeletal organization, and ARF-family-related transport. ARF, ADP-ribosylation factor; COPI, coat protein complex I; COPII, coat protein complex II; DAVID, Database for Annotation, Visualization and Integrated Discovery; ER, endoplasmic reticulum; L1CAM, L1 cell adhesion molecule; NCAM, neural cell adhesion molecule; PPI, protein–protein interaction; STRING, Search Tool for the Retrieval of Interacting Genes/Proteins.

base-derived hypotheses and should not be interpreted as evidence that these agents are effective treatments for *TMED3*-driven tumors.

Discussion

The functions of the *TMED* gene family and their mechanisms in regulating tumor development and progression remain incompletely understood. Beyond the *TMED3*-related mechanistic studies summarized in the Introduction, *TMED3* has also been implicated in breast cancer,[24] endometrial cancer,[25] osteosarcoma,[26] and chordoma.[27] Together with the established ER–Golgi transport role of TMED/p24-family proteins, these findings support the

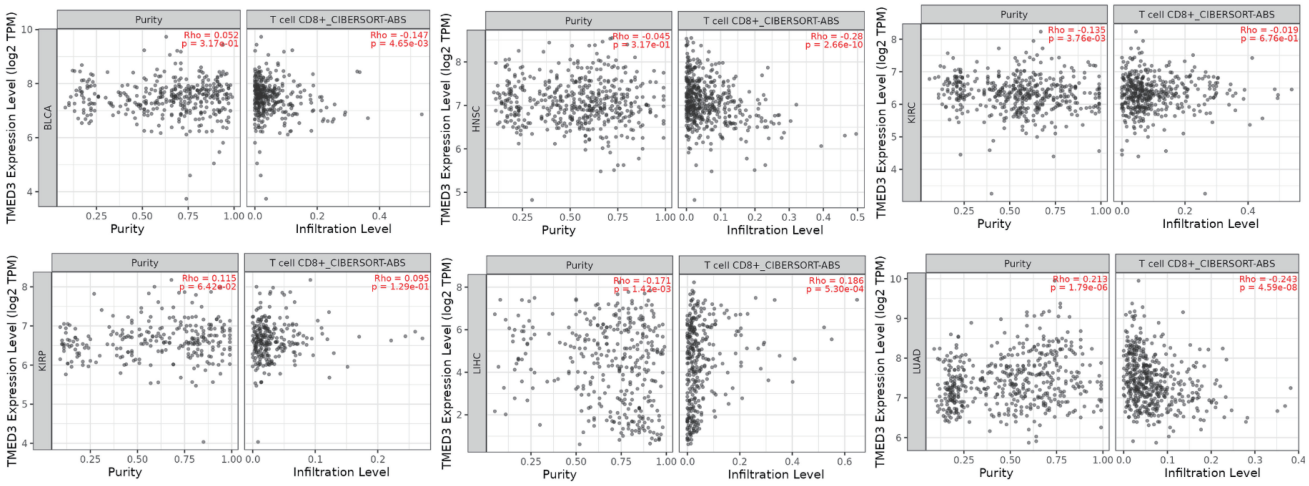

Fig. 7. Correlation between *TMED3* expression and estimated CD8⁺ T-cell infiltration in TIMER2.0 for BLCA, HNSC, KIRC, KIRP, LIHC, and LUAD. Each point represents a tumor sample; the fitted line and confidence band summarize the partial correlation reported by TIMER. Significant negative correlations were observed in BLCA, HNSC, and LUAD; correlations in KIRC and KIRP were not significant; and LIHC showed a positive correlation. Database-reported $P < 0.05$ was considered nominally significant. BLCA, bladder cancer; CD8, cluster of differentiation 8; CIBERSORT-ABS, absolute-mode CIBERSORT; HNSC, head and neck squamous cell carcinoma; KIRC, kidney renal clear cell carcinoma; KIRP, kidney renal papillary cell carcinoma; LIHC, liver hepatocellular carcinoma; LUAD, lung adenocarcinoma; TIMER2.0, Tumor Immune Estimation Resource 2.0; TPM, transcripts per million.

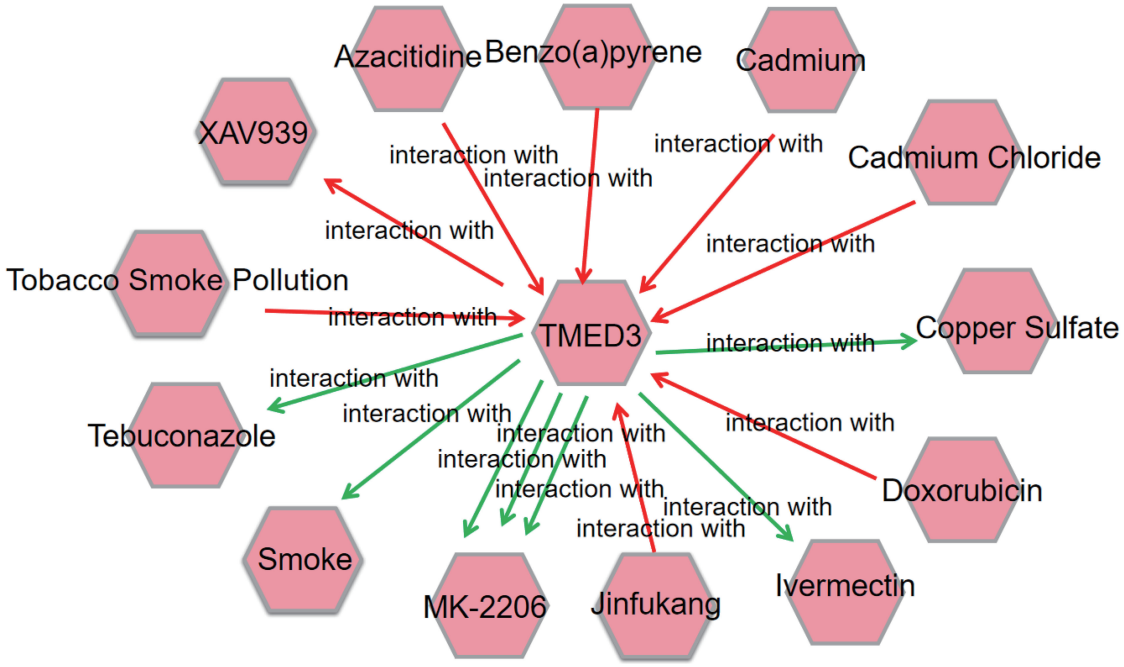

Fig. 8. CTD-derived chemical-gene interaction network for *TMED3* visualized in Cytoscape. Nodes include therapeutic compounds, environmental chemicals, and exposure-related agents. Red arrows indicate chemicals associated with increased *TMED3* expression, and green arrows indicate chemicals associated with decreased *TMED3* expression. The network is hypothesis-generating and does not establish causality or therapeutic efficacy. CTD, Comparative Toxicogenomics Database.

need for cancer-type-specific evaluation of *TMED3* rather than assuming a uniform cross-cancer function. In this study, *TMED3* expression was systematically assessed using public cross-cancer datasets, and the findings suggest that *TMED3* dysregulation may have prognostic relevance in several cancers. Importantly, the observed expression patterns were not fully uniform across analyses, particularly in KIRC subgroup-level results, indicating that tumor heterogeneity, dataset composition, and tumor-context-specific effects should be considered.[28]

TMED3 protein expression was also evaluated using HPA immunohistochemistry data. Higher TMED3 protein expression was observed in BLCA, HNSC, and LUAD tumor tissues compared with corresponding normal tissues, whereas clear protein-level upregulation was not observed in KIRC, LIHC, or KIRP. This partial concordance between transcript and protein results suggests that post-transcriptional regulation and tumor-level RNA–protein discordance may influence TMED3 assessment, in addition to antibody-based detection differences, sample heterogeneity, and database-specific limitations.[29,30] In addition, promoter methylation and CNVs were examined because epigenetic regulation and genomic alterations can affect gene expression in cancer.[31–33] The results suggest that promoter hypomethylation may be associated with increased *TMED3* expression in some cancer types, whereas CNV frequencies were generally low in the six cancers analyzed (Fig. 5). Therefore, methylation may be a more plausible regulatory mechanism than CNVs for *TMED3* expression in these datasets, although this conclusion requires independent methylation and expression validation.

PPI and pathway analyses indicated that *TMED3*-related genes are mainly involved in secretory pathway and vesicle transport processes, which is consistent with the canonical biological role of the transmembrane emp24 domain-containing/p24 family described above. $CD8^+$ T-cells are key mediators of antitumor immunity, but their infiltration and function can be altered during tumor progression and immune exhaustion.[34] In this study, *TMED3* expression showed significant negative correlations with $CD8^+$ T-cell infiltration in BLCA, HNSC, and LUAD, no significant correlations in KIRC and KIRP, and a positive correlation in LIHC, suggesting a cancer-type-specific immune association. These findings suggest that the immune association of *TMED3* may differ by cancer type and should not be interpreted as uniformly reflecting reduced antitumor immune infiltration.[35] However, the directionality and mechanism of this association cannot be determined from TIMER-based correlation analysis alone.

Chemical-gene interaction network analysis suggested that azacitidine and doxorubicin may be associated with increased *TMED3* expression, whereas MK-2206 may be associated with decreased *TMED3* expression. These CTD-derived findings are useful for generating hypotheses about potential regulatory relationships but should not be considered evidence that these drugs are clinically useful for *TMED3*-high tumors. Experimental studies are required to determine whether modulation of *TMED3* alters drug response and whether *TMED3* has any actionable therapeutic relevance.

Limitations

Several limitations should be acknowledged. First, this study is based entirely on public database mining and bioinformatics analysis; no *in vitro*, *in vivo*, or clinical sample-based experiments were performed to validate the biological function of *TMED3*. This is important because omics-based biomarker discovery generally requires rigorous independent validation before clinical translation.[36] Second, external validation was limited: GENT2 was used

for transcript-level validation, but protein expression, methylation, immune infiltration, and survival findings were not comprehensively validated in independent cohorts or platforms. Third, several analyses involved multiple comparisons across cancer types, molecular features, and clinical outcomes. Because only database-reported nominal *P*-values were consistently available and raw result matrices required for unified multiple-testing correction were not available from all platforms, adjusted q-values could not be calculated or reported. Therefore, the possibility of false-positive associations cannot be excluded, and the statistical findings should be interpreted as hypothesis-generating. Fourth, CTD-derived chemical-gene interactions are correlational or literature-curated associations and cannot establish therapeutic efficacy. Finally, discrepancies between databases, such as the KIRC expression pattern, highlight the need for standardized datasets, sensitivity analyses, and experimental confirmation before *TMED3* can be regarded as a clinically validated biomarker. In addition, post hoc sensitivity analyses could not be performed because the original raw datasets were not retrievable from all source platforms, further increasing uncertainty in the reported associations.

Conclusions

TMED3 is a cancer-type-specific prognostic candidate associated with shorter OS in HNSC, KIRC, KIRP, LIHC, and LUAD. Protein-level evidence shows higher expression in BLCA, HNSC, and LUAD, while promoter methylation and $CD8^+$ T-cell correlations provide testable regulatory and tumor microenvironment-related hypotheses. Because the analyses relied on database-reported nominal *P*-values without unified multiple-testing correction and lacked experimental validation, these findings establish *TMED3* as a priority candidate for independent mechanistic and clinical validation rather than a clinically validated biomarker or therapeutic target.

Acknowledgments

The authors thank UALCAN, Kaplan-Meier Plotter, GENT2, the Human Protein Atlas, MEXPRESS, cBioPortal, STRING, TIMER2.0, DAVID, and the Comparative Toxicogenomics Database for providing free access to their platforms.

Funding

This project was supported by the Shanghai Shenkang Hospital Development Center Medical-Enterprise Collaborative Innovation Project (SHDC2022CRT009).

Conflict of interest

The authors declare that they have no competing interests.

Author contributions

Study conception and design (ZK, LC), literature collection, manuscript organization (PJ, YY), data extraction, bioinformatics analysis, organization of results (JL), validation of the analytical workflow, interpretation of findings (XG, YL), drafting of the manuscript (ZK), study supervision, and critical revision of the manuscript for important intellectual content (LC). All authors reviewed and approved the final manuscript for submission.

Ethical statement

This study was based exclusively on publicly available, de-identified data obtained from UALCAN, Kaplan-Meier Plotter, GENT2, the Human Protein Atlas, MEXPRESS, cBioPortal, STRING, TIMER2.0, DAVID, and CTD. No new human specimens, animal experiments, clinical interventions, or identifiable private information were collected or analyzed by the authors. Therefore, institutional ethics approval and informed consent were not required.

Data sharing statement

The data supporting the findings of this study are publicly available and de-identified. They were obtained from the UALCAN database (http://ualcan.path.uab.edu), Kaplan-Meier Plotter (http://kmplot.com/analysis), GENT2 (http://gent2.appex.kr/), Human Protein Atlas (https://www.proteinatlas.org/), MEXPRESS (https://www.mexpress.be), cBioPortal (http://www.cbioportal.org), STRING (https://string-db.org/), TIMER2.0 (http://timer.cistrome.org/), DAVID (https://davidbioinformatics.nih.gov/), and the Comparative Toxicogenomics Database (CTD; http://ctdbase.org/).

References

[1] Bray F, Laversanne M, Sung H, Ferlay J, Siegel RL, Soerjomataram I, *et al*. Global cancer statistics 2022: GLOBOCAN estimates of incidence and mortality worldwide for 36 cancers in 185 countries. CA Cancer J Clin 2024;74(3):229–263. doi:10.3322/caac.21834, PMID:38572751.

[2] Zhou L, Li H, Yao H, Dai X, Gao P, Cheng H. TMED family genes and their roles in human diseases. Int J Med Sci 2023;20(13):1732–1743. doi:10.7150/ijms.87272, PMID:37928880.

[3] Strating JR, Martens GJ. The p24 family and selective transport processes at the ER-Golgi interface. Biol Cell 2009;101(9):495–509. doi:10.1042/BC20080233, PMID:19566487.

[4] Duquet A, Melotti A, Mishra S, Malerba M, Seth C, Conod A, *et al*. A novel genome-wide in vivo screen for metastatic suppressors in human colon cancer identifies the positive WNT-TCF pathway modulators TMED3 and SOX12. EMBO Mol Med 2014;6(7):882–901. doi:10.15252/emmm.201303799, PMID:24920608.

[5] Xie A, Xu X, Kuang P, Zhang L, Yu F. TMED3 promotes the progression and development of lung squamous cell carcinoma by regulating EZR. Cell Death Dis 2021;12(9):804. doi:10.1038/s41419-021-04086-9, PMID:34429402.

[6] Mishra S, Bernal C, Silvano M, Anand S, Ruiz i Altaba A. The protein secretion modulator TMED9 drives CNIH4/TGFα/GLI signaling opposing TMED3-WNT-TCF to promote colon cancer metastases. Oncogene 2019;38(29):5817–5837. doi:10.1038/s41388-019-0845-z, PMID:31253868.

[7] Chen X, Zhang W, Han X, Li X, Xia L, Wu Y, *et al*. TMED3 stabilizes SMAD2 by counteracting NEDD4-mediated ubiquitination to promote ovarian cancer. Mol Carcinog 2024;63(5):803–816. doi:10.1002/mc.23689, PMID:38411267.

[8] Wei X, Liang J, Huang H, Yang D, Wang X, Wang X, *et al*. TMED3 promotes prostate cancer via FOXO1a and FOXO3a phosphorylation. Oncol Res 2025;33(1):161–169. doi:10.32604/or.2024.048054, PMID:39735675.

[9] Qiao Y, Zhou L, Nie J, Li J, Hu Y, Gao P, *et al*. Transmembrane emp24 domain-containing protein 3 promotes the malignant progression of glioma by regulating the ZBTB7A signaling axis. Mol Biomed 2025;6(1):35. doi:10.1186/s43556-025-00274-7, PMID:40471367.

[10] Chandrashekar DS, Bashel B, Balasubramanya SAH, Creighton CJ, Ponce-Rodriguez I, Chakravarthi BVSK, *et al*. UALCAN: A Portal for Facilitating Tumor Subgroup Gene Expression and Survival Analyses. Neoplasia 2017;19(8):649–658. doi:10.1016/j.neo.2017.05.002, PMID:28732212.

[11] Chandrashekar DS, Karthikeyan SK, Korla PK, Patel H, Shovon AR, Athar M, *et al*. UALCAN: An update to the integrated cancer

data analysis platform. Neoplasia 2022;25:18–27. doi:10.1016/j.neo.2022.01.001, PMID:35078134.
[12] Lánczky A, Győrffy B. Web-Based Survival Analysis Tool Tailored for Medical Research (KMplot): Development and Implementation. J Med Internet Res 2021;23(7):e27633. doi:10.2196/27633, PMID:34309564.
[13] Park SJ, Yoon BH, Kim SK, Kim SY. GENT2: an updated gene expression database for normal and tumor tissues. BMC Med Genomics 2019;12(Suppl 5):101. doi:10.1186/s12920-019-0514-7, PMID:31296229.
[14] Uhlén M, Fagerberg L, Hallström BM, Lindskog C, Oksvold P, Mardinoglu A, *et al*. Proteomics. Tissue-based map of the human proteome. Science 2015;347(6220):1260419. doi:10.1126/science.1260419, PMID:25613900.
[15] Uhlen M, Zhang C, Lee S, Sjöstedt E, Fagerberg L, Bidkhori G, *et al*. A pathology atlas of the human cancer transcriptome. Science 2017;357(6352):eaan2507. doi:10.1126/science.aan2507, PMID:28818916.
[16] Koch A, Jeschke J, Van Criekinge W, van Engeland M, De Meyer T. MEXPRESS update 2019. Nucleic Acids Res 2019;47(W1):W561–W565. doi:10.1093/nar/gkz445, PMID:31114869.
[17] Cerami E, Gao J, Dogrusoz U, Gross BE, Sumer SO, Aksoy BA, *et al*. The cBio cancer genomics portal: an open platform for exploring multidimensional cancer genomics data. Cancer Discov 2012;2(5):401–404. doi:10.1158/2159-8290.CD-12-0095, PMID:22588877.
[18] Gao J, Aksoy BA, Dogrusoz U, Dresdner G, Gross B, Sumer SO, *et al*. Integrative analysis of complex cancer genomics and clinical profiles using the cBioPortal. Sci Signal 2013;6(269):pl1. doi:10.1126/scisignal.2004088, PMID:23550210.
[19] Szklarczyk D, Nastou K, Koutrouli M, Kirsch R, Mehryary F, Hachilif R, *et al*. The STRING database in 2025: protein networks with directionality of regulation. Nucleic Acids Res 2025;53(D1):D730–D737. doi:10.1093/nar/gkae1113, PMID:39558183.
[20] Shannon P, Markiel A, Ozier O, Baliga NS, Wang JT, Ramage D, *et al*. Cytoscape: a software environment for integrated models of biomolecular interaction networks. Genome Res 2003;13(11):2498–2504. doi:10.1101/gr.1239303, PMID:14597658.
[21] Sherman BT, Hao M, Qiu J, Jiao X, Baseler MW, Lane HC, *et al*. DAVID: a web server for functional enrichment analysis and functional annotation of gene lists (2021 update). Nucleic Acids Res 2022;50(W1):W216–W221. doi:10.1093/nar/gkac194, PMID:35325185.
[22] Li T, Fu J, Zeng Z, Cohen D, Li J, Chen Q, *et al*. TIMER2.0 for analysis of tumor-infiltrating immune cells. Nucleic Acids Res 2020;48(W1):W509–W514. doi:10.1093/nar/gkaa407, PMID:32442275.
[23] Davis AP, Wiegers TC, Sciaky D, Barkalow F, Strong M, Wyatt B, *et al*. Comparative Toxicogenomics Database's 20th anniversary: update 2025. Nucleic Acids Res 2025;53(D1):D1328–D1334. doi:10.1093/nar/gkae883, PMID:39385618.
[24] Zhang X, Luo Y, Li Q. TMED3 Promotes Proliferation and Migration in Breast Cancer Cells by Activating Wnt/β-Catenin Signaling. Onco Targets Ther 2020;13:5819–5830. doi:10.2147/OTT.S250766, PMID:32606792.
[25] Zhang J, Qi Y. Depleting TMED3 alleviates the development of endometrial carcinoma. Cancer Cell Int 2022;22(1):231. doi:10.1186/s12935-022-02649-0, PMID:35854294.
[26] Xu W, Li Y, Ye X, Ji Y, Chen Y, Zhang X, *et al*. TMED3/RPS15A Axis promotes the development and progression of osteosarcoma. Cancer Cell Int 2021;21(1):630. doi:10.1186/s12935-021-02340-w, PMID:34838013.
[27] Yang J, Huang H, Xiao D, Duan Y, Zheng Y, Chen Z. Knockdown of TMED3 inhibits cell viability and migration and increases apoptosis in human chordoma cells. Int J Oncol 2021;58(5):15. doi:10.3892/ijo.2021.5195, PMID:33760171.
[28] Lawrence MS, Stojanov P, Polak P, Kryukov GV, Cibulskis K, Sivachenko A, *et al*. Mutational heterogeneity in cancer and the search for new cancer-associated genes. Nature 2013;499(7457):214–218. doi:10.1038/nature12213, PMID:23770567.
[29] Vogel C, Marcotte EM. Insights into the regulation of protein abundance from proteomic and transcriptomic analyses. Nat Rev Genet 2012;13(4):227–232. doi:10.1038/nrg3185, PMID:22411467.
[30] Zhang Y, Chen F, Chandrashekar DS, Varambally S, Creighton CJ. Proteogenomic characterization of 2002 human cancers reveals pan-cancer molecular subtypes and associated pathways. Nat Commun 2022;13(1):2669. doi:10.1038/s41467-022-30342-3, PMID:35562349.
[31] Teschendorff AE, Relton CL. Statistical and integrative system-level analysis of DNA methylation data. Nat Rev Genet 2018;19(3):129–147. doi:10.1038/nrg.2017.86, PMID:29129922.
[32] Pan H, Renaud L, Chaligne R, Bloehdorn J, Tausch E, Mertens D, *et al*. Discovery of Candidate DNA Methylation Cancer Driver Genes. Cancer Discov 2021;11(9):2266–2281. doi:10.1158/2159-8290.CD-20-1334, PMID:33972312.
[33] Beroukhim R, Mermel CH, Porter D, Wei G, Raychaudhuri S, Donovan J, *et al*. The landscape of somatic copy-number alteration across human cancers. Nature 2010;463(7283):899–905. doi:10.1038/nature08822, PMID:20164920.
[34] Philip M, Schietinger A. CD8(+) T cell differentiation and dysfunction in cancer. Nat Rev Immunol 2022;22(4):209–223. doi:10.1038/s41577-021-00574-3, PMID:34253904.
[35] Bruni D, Angell HK, Galon J. The immune contexture and Immunoscore in cancer prognosis and therapeutic efficacy. Nat Rev Cancer 2020;20(11):662–680. doi:10.1038/s41568-020-0285-7, PMID:32753728.
[36] Glaab E, Rauschenberger A, Banzi R, Gerardi C, Garcia P, Demotes J. Biomarker discovery studies for patient stratification using machine learning analysis of omics data: a scoping review. BMJ Open 2021;11(12):e053674. doi:10.1136/bmjopen-2021-053674, PMID:34873011.